22nd International Workshop on Water Waves and Floating Bodies, 15th–18th April 2007, Plitvice

POWER CONVERSION IN THE ANACONDA WEC

J.R. Chaplin
University of Southampton, UK
j.r.chaplin@soton.ac.uk

F.J.M. Farley
Maritime Energy Developments Ltd, France
farley@bulgewave.com

R.C.T. Rainey
Atkins Oil and Gas Division, London, UK
rod.rainey@atkinsglobal.com

INTRODUCTION

The Anaconda all-rubber WEC operates in a completely new way, transferring energy from water waves to bulge waves in a giant water-filled submerged rubber tube, aligned head-to-sea. Initial indications are that it offers advantages of low capital and operational costs, owing to its extreme simplicity and the unique durability of rubber (see www.bulgewave.com).

This paper presents briefly the results of the first series of laboratory tests carried out on a model of the device, providing evidence of a capture width of between 3 and 4 diameters over a wide range of frequencies. Secondly we discuss a concept for a simple power take-off system.

LABORATORY EXPERIMENTS

These experiments were aimed at exploring some of the basic hydrodynamic features of the Anaconda. The model tube, about 2.5m long and 78mm in diameter, was made from rubber sheet 0.15mm thick. Its Young's modulus E and loss coefficient β in the stress/strain relation $\sigma = E(\varepsilon + \beta\dot{\varepsilon})$ were approximately E = 1.9MPa and β = 0.0059s. The tube was installed at an elevation just below still water level on the centre-line of a wave flume 0.42m wide, 18m long, with a still water depth of 0.7m. Figure 1 shows the model in place, responding to waves coming from the left.

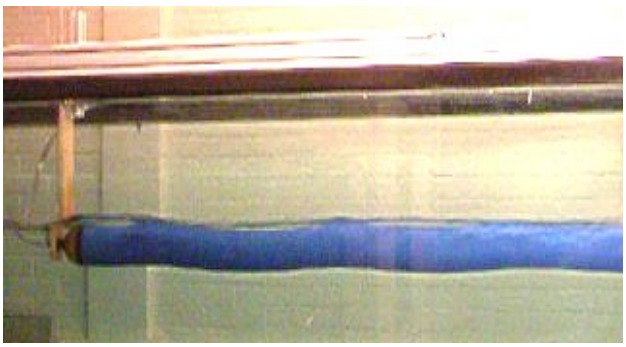

Fig. 1. The leading part of the Anaconda model in the wave flume. The rubber is slightly buoyant.

In these experiments, the tube was pressurised to an excess head of about 70mm, and then sealed. A transducer recorded the internal pressure at one end. Regular waves could be generated in the tank with a flap-type wavemaker with active absorption, and those that passed the Anaconda model were efficiently dissipated in a vertical wedge of firm poly-ether foam from which reflections are less than 3%. Wave gauges recorded water surface elevations ahead and behind the model. In some cases the leading end of the model was mounted not on a fixed arm (as shown in fig. 1) but on the carriage of a linear actuator that could be oscillated in the vertical direction. Otherwise both ends of the tube were stationary.

Three types of measurements were carried out: bulge wave speeds in the tube in air and in still water, pressures at one end of the tube when the other end was oscillated vertically in still water, and pressures at the downwave end in regular waves.

Bulge wave speed

Initial estimates of bulge wave speed were made from observations of bulges started by hand, propagating along a water-filled tube lying on a horizontal surface in air. In these conditions the cross section of the tube was inevitably non-circular, but measured speeds were within 10% of the theoretical value for a circular tube of the same area. Theoretically the bulge wave speed c (in the absence of hysteresis, which

has a weak effect on it) is equal to $(\rho D)^{-1/2}$, where D is the distensibility (Lighthill, 1978, Sect.2.2). For a circular tube of diameter d and wall thickness h, the distensibility $D = d/Eh$.

In the wave flume, with one end of the model mounted on the actuator, small bulge waves could be launched along the tube in still water by driving the vertical carriage with a step input of very small amplitude. The pressure transducer at the other end clearly recorded the arrival of the resulting bulge wave, and the measurements indicated a speed of 1.36m/s. The theoretical speed was $(\rho D)^{-1/2}$ = 1.93m/s. It seems reasonable to link the difference in this case to the presence of the surrounding water.

Forced vertical oscillations in still water

It is argued by Farley & Rainey (2006a) that their theory of bulge waves driven by water waves, derived for the case of a straight horizontal submerged tube, applies equally to the case of a tube which undulates in the vertical plane, following the free surface. In fact when mounted close to the surface in waves, the tube does respond with a vertical motion, generally following the free surface but with a phase lag; see fig. 1. Farley & Rainey's proposition is that to a first approximation, the effect of the internal hydrostatic pressure variation in this case is equivalent to that of the equal and opposite pressure variation outside a tube that remains straight.

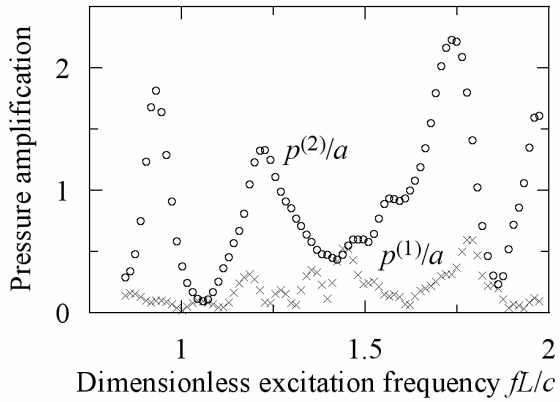

Figure 2. Normalised amplitudes of the first and second frequency components of the pressure measured at the stationary end of the tube when it was oscillated vertically at the other end in still water. In this case the amplitude of the oscillation a was one-half of the tube's diameter d.

Experiments were carried out to test this idea in a closely related situation, namely that in which one end of the tube (well submerged) was oscillated vertically at small amplitudes in still water. Bulge waves generated by this motion were apparent in the time series of internal pressures recorded at the other (stationary) end of the tube.

Except at extremely small amplitudes of motion, the measured pressures were dominated by a component oscillating at twice the driving frequency. This suggests that bulge waves were generated by the vertical motion, but were predominantly caused by a distortion of the tube's cross section that must occur in the same sense on both upwards and downwards strokes. As expected, the amplitude of the double frequency pressure signal was predominantly proportional to the square of the amplitude of the driving motion.

The amplitudes of pressures recorded at the stationary end of the tube were quite large. In fig. 2, for cases in which the amplitude a of the driven vertical motion was one-half of the tube's diameter, the pressure amplifications $p^{(1)}/a$ and $p^{(2)}/a$ at the first two frequencies are plotted as functions of the dimensionless excitation frequency fL/c, where f is the frequency of the motion and L the length of the tube. Peak pressure amplifications exceed 2. But for reasons that are not clear, peak responses do not occur at frequencies related in obvious ways to the characteristic frequency c/L.

Measurements in waves

In these experiments we recorded pressures and water surface elevations, for each of a number of wave frequencies, and at each wave frequency at three wave amplitudes. Since the tube was closed at each end and not fitted with any power take-off system, the wave energy it absorbed was accounted for by hysteresis losses in the rubber, and (probably much smaller) losses in the internal flow.

In the upper plot of fig. 3 is shown the internal pressure amplification at the downwave end of the tube as a function of the ratio of the tube length L to the water wavelength λ. The pressure amplification is the amplitude of the bulge pressure at the water wave frequency divided by the amplitude of the incident

water wave-induced pressure at the same elevation. (Contributions at higher frequencies in this case appeared to be much smaller.) There are discernable peaks at $L/\lambda = 1$ and 2, suggesting standing bulge waves. There is also a peak at $L/\lambda = 2.75$, at which the water wave speed coincides with the free bulge wave speed.

The lower plot in fig. 3 presents two estimates of capture widths. Those plotted with crosses were calculated from measurements of incident, reflected and transmitted waves. Those plotted with open circles represent the energy losses in the rubber over the entire length of the tube, calculated from the damped bulge wave equation

$$\frac{\partial^2 p_b}{\partial t^2} - \beta \frac{\partial^3 p_b}{\partial t^3} = \frac{1}{\rho D} \frac{\partial^2}{\partial x^2}\left(p_b + p_w\right)$$

(Farley & Rainey, 2006b), where $p_b(x,t) + p_w(x,t)$ is the pressure inside the tube: p_w is the external pressure, and p_b the excess internal pressure that is supported by tension in the tube wall.

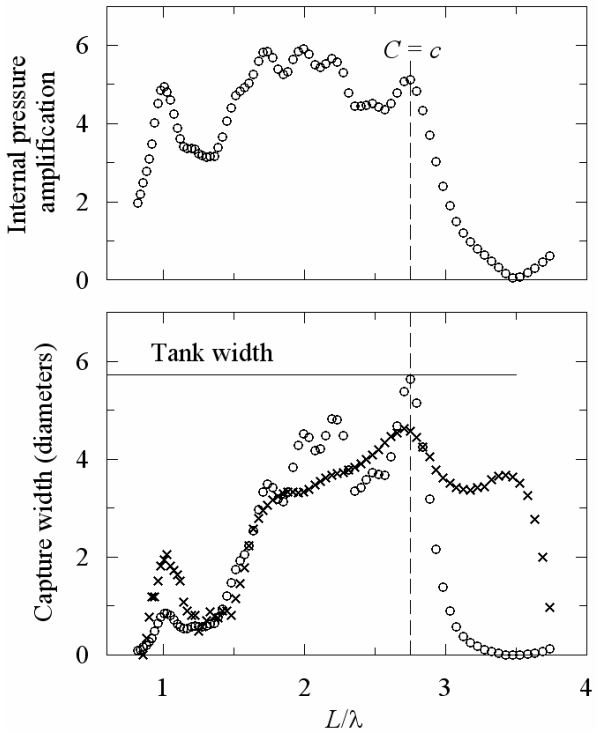

Figure 3. (Above) pressure amplification at the downwave end of the tube in waves; (below) estimates of capture widths obtained from wave (crosses) and pressure (circles) measurements.

Pressures at all points along the tube were estimated by using this equation with appropriate closed end boundary conditions, and by matching the pressure at the downwave end of the tube with the measurements. From the resulting hoop stresses it was then possible to calculate hysteresis losses and the associated capture width. In the resulting plot of capture widths (fig. 3), some peaks can be associated with coincidences of the tube's length L with integer multiples of the water wavelength λ, while the greatest capture width (very close to the entire width of the tank) occurs when the water wave speed C equals the free bulge wave speed c.

Conclusions

These measurements support the view that the Anaconda is a very promising device that warrants further study. Estimated capture widths exceed three diameters over a wide range of wave frequencies. However, there are clearly some hydrodynamic features that are not well understood, and which raise interesting and novel questions.

POWER TAKE-OFF

The bulge wave power can be extracted in many ways (e.g. the hysteresis in the rubber extracts power all along the device – as in the experiments), but the simplest option is to absorb the power at the tail. For efficient conversion, it is usually beneficial to smooth the power initially with accumulators. For a device on the seabed, this can be accomplished with one-way valves to high and low pressure accumulators, see fig. 4. A turbine (not shown) then operates in the smoothed flow between the accumulators.

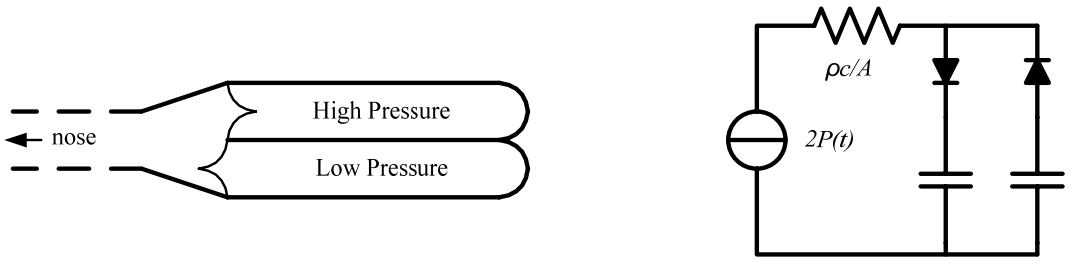

Figure 4

The equivalence between one-dimensional waves and electrical circuits is well-known (see e.g. Lighthill, 1978, p.104) – voltage is an analogue of pressure, and current is an analogue of volume flow rate. If the incoming bulge wave has a pressure $P(t)$ at the tail, and the reflected bulge wave has a pressure $R(t)$, then the total pressure $T(t)$ at the tail is $P(t) + R(t)$. If the cross-sectional area of the tube is A, and we assume that the incoming bulge wave is travelling at its free propagation speed c, then the volume flows is (Lighthill, 1978, p.94):

$$P(t)/(\rho c/A) - R(t)/(\rho c/A) = \{2P(t) - (P(t) + R(t))\}/(\rho c/A) = \{2P(t) - T(t)\}/(\rho c/A)$$

Thus the equivalent circuit is as shown in fig. 4, where the valves and accumulators are represented by diodes and capacitors. Assuming a sinusoidal incoming bulge wave and large capacitors (accumulators), the power absorption is readily calculated as a matter of electrical engineering – it reaches a maximum of 92.3% of the incident bulge-wave power, if the accumulators are set to plus and minus 80% of the peak value of $P(t)$. And it remains over 50%, if they are set between between 24% and 146% of it. The reflected wave (which will be re-reflected at the nose, so its power is not lost) is readily obtained too - at 92.3% absorption it is all higher harmonics – the 3rd and 5th have 6.7% and 0.8% of the incident power.

For floating versions of the device, the seabed is not available as a fixed reference. Instead, an additional length of non-distensible tube can be added, as an inertial reference.

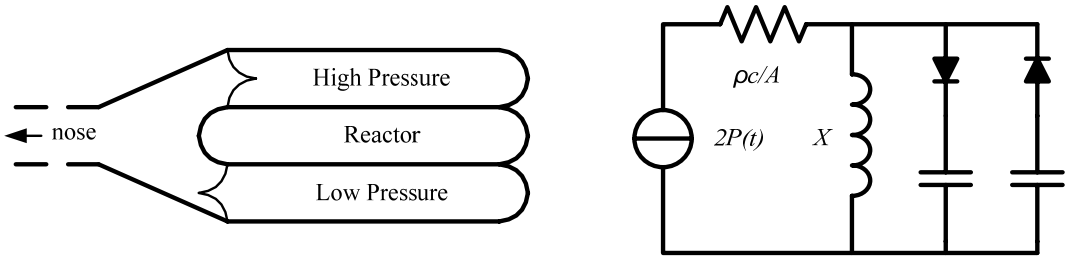

Figure 5

This modifies the equivalent circuit as shown in fig. 5. (Note that a free end is zero reactance and thus a short circuit.) If the length of this additional tube is $\lambda/2\pi$ (λ = wavelength), then its reactance X will have the same impedance $\rho c/A$ as the main tube. Thus a moderate additional length of tube is sufficient to make a good inertial reference, and give comparable performance to a seabed-mounted device.

REFERENCES

Lighthill, M.J. (1978) Waves in Fluids. CUP.

Farley, F.J.M. and Rainey, R.C.T. (2006a) Radical design options for wave-profiling wave energy converters. IWWWFB06.

Farley, F.J.M. and Rainey, R.C.T. (2006b) Bulge wave theory with hysteresis. Unpublished note.